# P2-26 Spatial Profile Fidelity of Incoherent-to-Coherent Conversion based on Photorefractive Two-Wave Mixing

Huitian Wang, Jiasen Zhang, Shin Yoshikado, and Tadashi Aruga
Communications Research Laboratory, Ministry of Posts and Telecommunications
4-2-1 Nukui-Kitamachi, Koganei-City, Tokyo 184-8795, Japan
Phone: +81-42-327-5398, Fax: +81-42-327-6658, E-mail: htwang@crl.go.jp

## Introduction

Photorefractive materials are of interest for a variety of potential applications. One application is to perform the conversion of an incoherent image into its coherent replica, as a spatial light modulator (SLM) in coherent optical information processing. Since Kamshilin and Petrov[1] proposed a photorefractive SLM in 1980, several kinds of incoherent-to-coherent converters (ITCC's) have been developed[2-4]. In these devices one coherent reading beam is required and the generated coherent image may be a negative/positive replica of the incoherent input image. Recently, we demonstrated a new ITCC using the photorefractive fanning effect[5]; this is an effective and simple method because there are only two beams (an incoherent image beam and a uniform coherent beam) and no reading beam is required. For all ITCC's, they have a common point that an incoherent image beam selectively erases (or rather modulates) a uniform volume grating.

The spatial profile fidelity of the coherent output image for ITCC must depend on various factors, such as the intensity ratios of incoherent beam to coherent beams, the properties of the photorefractive medium, and the geometric configuration. Therefore, it is absolutely necessary to clarify the dependence of spatial profile fidelity on the various factors in order to obtain the best output images, which is our propose. In this paper, we concentrate on the spatial profile fidelity for incoherent-to-coherent conversion based on the two-wave mixing in a photorefractive crystal.

## Theoretical Formulas

In a photorefractive crystal, there always occurs non-reciprocal exchange of energy between two coherent beams. Thus a beam can be depleted while another can be amplified. If the crystal is also illuminated by incoherent image beam at the same time, the volume index grating formed by the two coherent beams will be modulated. As a result, the depleted or amplified beam should bear a positive or negative replica of the spatial information of the incoherent image, respectively.

For the sake of simplicity, here we treat only the two-dimensional case in the *xoz*, and assume that the crystal has an infinite dimension in the $x$ direction and a finite length of $L$ along the $z$ direction, as Fig. 1. Three input beams, two uniform coherent beams (beam 1 and beam 2) and one incoherent image beam (beam 3), enter the crystal from the same side at $z = 0$. We

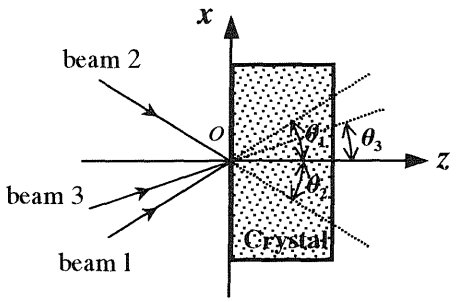


Figure 1 Geometric configuration of incoherent-to-coherent conversion.

assume that the three beams have a common angular frequency $\omega$. The total electric field $E(x, z)$ inside the photorefractive crystal can be written

$$E(x,z) = \frac{1}{2}\{\sum_{m=1}^{3} A_m(x,z)e^{jk(x\sin\theta_m + z\cos\theta_m)} + c.c.\}, \quad (1)$$

where $A_m$ and $\theta_m$ are the amplitude distribution and the incident angle of beam $m$, respectively; $k = \omega n_o/c$, $n_o$ is the background refractive index of the photorefractive crystal when no light is present, $c$ is velocity of light in vacuum. Under the slowly-varying field approximation, we can derive the following steady-state coupled wave equations in the absence of absorption

$$\frac{\partial A_1}{\partial z} = -\frac{\gamma}{\cos\theta_1}\frac{A_1 A_2^*}{|A_1|^2 + |A_2|^2 + |A_3|^2}A_2,$$
$$\frac{\partial A_2}{\partial z} = -\frac{\gamma^*}{\cos\theta_2}\frac{A_1^* A_2}{|A_1|^2 + |A_2|^2 + |A_3|^2}A_1, \quad (2)$$

where $\gamma = jkn_1 e^{-j\phi}/2n_o$, $n_1$ is a real and positive number and $\phi$ is the phase shift.

We use numerical method to solve Eq. (2) and let the amplitudes of the input fields for the three beams as

$$A_1(x,0) = 1, A_2(x,0) = \sqrt{\beta},$$
$$A_3(x,0) = \sqrt{\rho}\sum_{\nu=-1}^{1}\mathrm{rect}\left(\frac{x-2\nu}{d}\right), \quad (3)$$

where $\beta$ and $\rho$ are the intensity ratios of beam 2 to beam 1 and beam 3 to beam 1 at $z = 0$, respectively.

In the numerical calculations, we have taken (i) $n_o \approx 2.42$ at $\lambda = 532$ nm and $\phi = \pi/2$ (as $BaTiO_3$), (ii) $\theta_1 = -\theta_2 = 6°$, and (iii) the transverse points within the range $-3d \le x \le 3d$ and the number of longitudinal steps as 1024. To evaluate the quality of the coherent output images bore by beams 1 and 2, it is necessary to introduce the spatial profile fidelity as

$$F_1 = \frac{\int |A_1(x,L)| \cdot |A_3(x,0)|\, dx}{\left(\int |A_1(x,L)|^2\, dx \cdot \int |A_3(x,0)|^2\, dx\right)^{1/2}}, \tag{4a}$$

$$F_2 = \frac{\int |A_2(x,L)| \cdot |\sqrt{\rho} - A_3(x,0)|\, dx}{\left(\int |A_2(x,L)|^2\, dx \cdot \int |\sqrt{\rho} - A_3(x,0)|^2\, dx\right)^{1/2}}. \tag{4b}$$

**Results of Simulation**

Figure 2 shows the dependence of $F_1$ and $F_2$ on the incident angle $\theta_3$ at different $\beta$ when $\rho = 1$, $\gamma = 3$ mm$^{-1}$, $L = 1$ mm, and $d = 0.05$ mm. The results indicate that, in order to produce the best positive/negative coherent output images the image beam 3 must be propagated along the same direction relative to beam 1/2 and $\beta$ must have a proper value ($\beta = 1$ for positive image while $\beta$ is smaller than $10^{-4}$ for negative image). Note that in all the calculations below we take $\theta_3 = \theta_1$ and $\beta = 1$ for $F_1$ while $\theta_3 = \theta_2$ and $\beta = 10^{-5}$ for $F_2$.

Figure 3 plots variations of $F_1$ and $F_2$ with $\rho$ at various $\gamma$. $F_1$ increases to achieve a limit value with the increase of $\rho$; for large $\gamma$, $F_1$ can achieve its limit value when $\rho = 2$. If $\gamma$ is small, $F_2$ increases to achieve a limit value with the increase of $\rho$; whereas if $\gamma$ is large $F_2$ increases to a maximum value at $\rho = 2$ and then slowly decreases. So, to obtain the best coherent output images, if the crystal has a large $\gamma$ the optimum value of $\rho$ should be 2, whereas $\rho$ must have a larger value.

Figure 4 shows $F_1$ and $F_2$ as functions of $L$ at different $\gamma$ when $\rho = 3$. In order to obtain the best coherent output images, for a crystal with a small $\gamma$, its length must be long, while for a crystal with large $\gamma$, its length should be short.

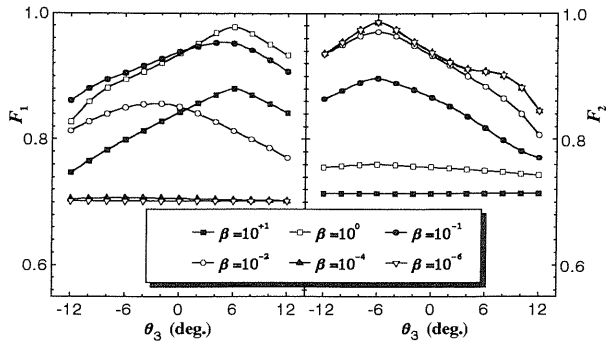


Figure 2 An example of the dependence of $F_1$ and $F_2$ on $\theta_3$ for the several different values of $\beta$.

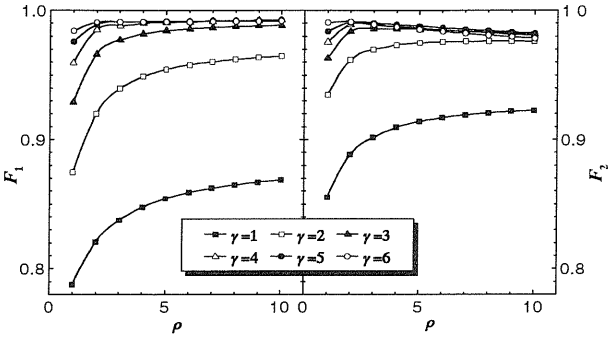


Figure 3 Variation of $F_1$ and $F_2$ with $\rho$ at different values of $\gamma$.

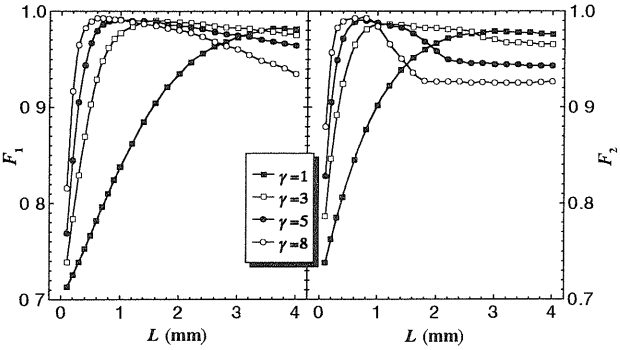


Figure 4 Dependence of $F_1$ and $F_2$ on the length of the crystal for different values of $\gamma$.

**Conclusion**

We have analyzed numerically the dependence of coherent output images on some parameters for ITCC. The calculated results point out that the best coherent output images can be obtained when (a) the incoherent image is propagated in the same direction as the corresponding coherent beam, (b) the intensity ratio $\beta$ of the two coherent beams should be unity for positive images while be smaller than $10^{-4}$ at least for negative images, (c) $\rho$ should be to 2 and $L$ should be shorter for the case of large $\gamma$, while $\rho$ must be larger and $L$ must be longer for small $\gamma$.

**References**


1. A. A. Kamshilin and M. P. Petrov, Soc. Tech. Phys. Lett. 6 (1980) 144.
2. J. Ma, L. Liu, S. Wu, Z. Wang, and L. Xu, Opt. Lett. 14 (1989) 572.
3. E. Voit and P. Gunter, Opt. Lett. 12 (1987) 769.
4. A. Marrakchi, Opt. Lett. 13 (1988) 654.
5. J. Zhang, H. Wang, S. Yoshikado, and T. Aruga, Opt. Lett. 22 (1997) 1612.